

Shadowing-Based Antenna Selection for V2V Communications

Petros S. Bithas
Department of Digital Systems,
University of Piraeus, Greece
Email: pbithas@unipi.gr

Athanasios G. Kanatas
Department of Digital Systems,
University of Piraeus, Greece
Email: pbithas@unipi.gr

David W. Matolak
Department of Electrical Engineering,
University of South Carolina, Columbia,
SC 29208 USA
Email: matolak@cec.sc.edu

Abstract—Antenna selection (AS) is considered as an ideal approach for improving the performance of vehicle-to-vehicle (V2V) communications, while satisfying the hardware and power limitations that exist in vehicles. However, the promised gain over single antenna schemes is affected by the fast varying wireless channel, since AS is frequently performed using outdated versions of the signal-to-noise ratio. In this paper, we propose an AS scheme that exploits the stationarity of large scale fading. In particular, by adopting shadowing information as an AS criterion, the negative consequences of the outdated channel state information (CSI) can be alleviated, since large-scale fading varies more slowly as compared to small-scale fading. The performance of the proposed technique is analyzed using the criterion of outage probability. It is shown that the new scheme outperforms the corresponding one that is based on outdated CSI, especially in scenarios with mild channel conditions, in terms of fading/shadowing severity. Moreover, empirical results have been used to verify the effectiveness of the considered shadowing model.

I. INTRODUCTION

In V2V communications, due to the continuous motion of the Tx, Rx, and the surrounding scatterers, the channel conditions can change rapidly. Thus, an antenna selection (AS) system that chooses antennas using channel state information (CSI) in practice operates using outdated versions of CSI. As a result, irreducible diversity gain losses are expected, as it has been shown in many studies in the past, e.g., [1], [2]. The performance degradation due to the outdated CSI increases with the speed of vehicle, since higher Doppler shifts arise, which, in limiting scenarios, will result to performance similar to that in single antenna communication systems.

A promising solution to improve this situation is proposed in [3], where a transmit antenna selection (TAS) scheme based on shadowing information (SI) was proposed. In that system, the transmit antenna offering the largest amplitude shadowing variable between the Tx and the Rx is selected. It was shown that as the number of antennas increases, the shadowing consequences on the transmitted signal can be eliminated. The same basic idea was recently adopted in [4], [5] in physical layer security and cooperative relaying scenarios, respectively. For example, in [5], it was also shown that SI-based AS is a promising option for communication systems

operating in higher frequencies, e.g., in extremely higher frequency bands. A common observation in all the previously mentioned works is that the exploitation of the SI provides worth-studying opportunities toward designing low complexity communication techniques that offer similar performance with existing CSI-based ones. Here, it should be noted that the shadowing effects, which are induced by obstructing vehicles between Tx and Rx, considerably affect the performance of intervehicular communication systems [6], [7]. However, very few contributions have analytically investigated the impact of large scale fading in these systems and the required countermeasures for improving their performance.

Motivated by the aforesaid observations, in this paper, we propose and analytically investigate a TAS/selection diversity (SD) system that exploits stationarity of large scale fading. The system operates in a composite fading environment, in which small-scale fading and shadowing are modeled using the Rice and the Inverse-Gamma (IG) distributions, respectively. The latter distribution has been recently proposed as an alternative distribution for accurately modeling the shadowing variable variations [8], [9]. Based on this model, mathematically convenient statistical expressions can be derived, in contrast to the cumbersome expressions that are obtained with the lognormal distribution. In this context, important statistical characteristics for the Rice/IG composite model are derived in closed form for a single-input single-output (SISO) communication system. The analysis is then extended to the scenario where multiple antennas exist at both the Tx and the Rx, and the pair that offers the largest amplitude shadowing variable is selected for the communication phase¹. In the derived results, the generic case where independent but non-identically distributed (i.n.d.) fading/shadowing conditions exist is considered. Simplified expressions are also provided for independent and identically distributed (i.i.d.) conditions. Both these scenarios have been studied in order to prepare a reference point. Finally, the empirical data that

¹Since the shadowing variables vary much more slowly than the received SNR, it is reasonable to assume that their values at the selection and the reception phases are fully (temporally) correlated.

have been also employed verify the appropriateness of the IG distribution to model shadowing variations.

The remainder of the paper is organized as follows. In Section II, the system and channel models of the scheme under consideration are presented. In Section III, a statistical framework for the received SNR has been developed. In Section IV, representative numerical evaluated results and comparisons with measured data are presented and discussed, while in Section V, the concluding remarks can be found.

II. SYSTEM AND CHANNEL MODEL

A. System Model

We consider a low complexity communication system in which both the Tx and the Rx are equipped with one RF chain and N_t, N_r antennas, respectively. The links between the Tx and the Rx are simultaneously affected by both small-and large-scale fading. The received SNR between the Tx antenna i and Rx antenna j is given by

$$\gamma_{i,j} = h_{i,j}^2 s_{i,j}^2 \frac{E_s}{N_0} = g_{i,j} p_{i,j}, \quad (1)$$

where $h_{i,j}, s_{i,j}$ denote the fading and shadowing variables, respectively, $g_{i,j} = h_{i,j}^2, p_{i,j} = s_{i,j}^2 \frac{E_s}{N_0}$, E_s is the average energy per transmitted symbol, and N_0 the power spectral density of the additive white Gaussian noise. In traditional CSI-based AS schemes operating in time-varying mobile communication environments, the estimated channel condition at the selection phase could be significantly different from the corresponding one at the reception instance, due to the fast variations of the wireless medium. In particular, even in the ideal scenario where the feedback interval T_D is equal to or less than channel's coherence time T_c , i.e., the duration within the channel is approximately constant, a delayed version of the CSI will be available. An alternative approach is to select the antenna based on information that depends on the shadowing conditions [3]. This approach is actually based on the fact that the decorrelation distance of the large scale fading is approximately two orders of magnitude larger than the one of the small-scale fading [10], for current frequency bands of interest. Therefore, with SI-based AS, the antennas pair that is selected is the one providing the maximum averaged received power, i.e., shadowing variable, over a predetermined time interval. After the antenna-pair selection is performed, the corresponding index is fed back to the Tx in order to proceed with the signal transmission. Thus, given that the ℓ, κ th antennas pair is selected, the received SNR can be expressed as

$$\gamma_{\ell,\kappa} = g_{\ell,\kappa} \max_{\substack{1 \leq i \leq N_t \\ 1 \leq j \leq N_r}} \{p_{i,j}\} = g_{\ell,\kappa} p_{\max}, \quad (2)$$

where $g_{\ell,\kappa}$ depends on the small-scale fading of the selected pair. It is worth-noting that $g_{\ell,\kappa}$ s change in every channel's coherence time, whereas $p_{i,j}$ s do not.

B. Channel Model

We consider the scenario where line-of-sight (LoS) conditions co-exist with large-scale variations caused by shadowing from large objects, e.g., other vehicles [11]. Therefore, Rice and IG distributions have been employed to model small scale fading and shadowing variations, respectively. The probability density function (PDF) of $g_{i,j}$ is given by [12, eq. (2.16)]

$$f_{g_{i,j}}(x) = \frac{(k_{i,j} + 1)}{\Omega} \exp\left(-k_{i,j} - \frac{(k_{i,j} + 1)x}{\Omega}\right) \times I_0\left(2\sqrt{\frac{k_{i,j}(k_{i,j} + 1)x}{\Omega}}\right), \quad (3)$$

where $k_{i,j}$ corresponds to the ratio of the power of the specular component to the average power of the scattered component, $\Omega = \mathbb{E}\langle g_{i,j} \rangle$, with $\mathbb{E}\langle \cdot \rangle$ denoting expectation, and $I_v(\cdot)$ denotes the modified Bessel function of the first kind and order v [13, eq. (8.406/1)]. Similar to [8], the shadowing variables $p_{i,j}$ are assumed to follow IG distribution, with PDF given by

$$f_{p_{i,j}}(y) = \frac{\bar{\gamma}_{i,j}^{\alpha_{i,j}}}{\Gamma(\alpha_{i,j}) y^{\alpha_{i,j}+1}} \exp\left(-\frac{\bar{\gamma}_{i,j}}{y}\right), \quad (4)$$

where $\alpha_{i,j} > 1$ is the shaping parameter of the distribution, related to the severity of the shadowing, $\bar{\gamma}_{i,j}$ denotes the scaling parameter, related to the average received SNR, and $\Gamma(\cdot)$ is the gamma function [13, eq. (8.310/1)]. Using the total probability theorem, the PDF of the instantaneous received SNR of the i, j th pair, $\gamma_{i,j}$, is given by

$$f_{\gamma_{i,j}}(\gamma) = \int_0^\infty f_{g_{i,j}}(\gamma|y) f_{p_{i,j}}(y) dy. \quad (5)$$

Substituting (3) and (4) in (5) and using [13, eq. (6.643/2)], the following expression for the PDF of $\gamma_{i,j}$ is derived

$$f_{\gamma_{i,j}}(\gamma) = \frac{(k_{i,j} + 1)^{1/2} \exp(-k_{i,j}) \bar{\gamma}_{i,j}^{\alpha_{i,j}} \alpha_{i,j}}{\sqrt{k_{i,j} \bar{\gamma}} [(k_{i,j} + 1)\gamma + \bar{\gamma}_{i,j}]^{\alpha_{i,j}+1/2}} \times \exp\left[\frac{k_{i,j}(k_{i,j} + 1)\gamma}{2((k_{i,j} + 1)\gamma + \bar{\gamma}_{i,j})}\right] \times M_{-\alpha_{i,j}-\frac{1}{2}, 0}\left[\frac{k_{i,j}(k_{i,j} + 1)\gamma}{(k_{i,j} + 1)\gamma + \bar{\gamma}_{i,j}}\right], \quad (6)$$

where $M_{\kappa,\mu}(\cdot)$ denotes the Whittaker function [13, eq. (9.220/2)]. The corresponding cumulative distribution function (CDF) expression is given by

$$F_{\gamma_{i,j}}(\gamma) = \frac{(k_{i,j} + 1)\gamma}{(k_{i,j} + 1)\gamma + \bar{\gamma}_{i,j}} \exp\left[-\frac{k_{i,j} \bar{\gamma}_{i,j}}{(k_{i,j} + 1)\gamma + \bar{\gamma}_{i,j}}\right] \times \sum_{k_1=0}^{\alpha_{i,j}-1} \left[\frac{\bar{\gamma}_{i,j}}{(k_{i,j} + 1)\gamma + \bar{\gamma}_{i,j}}\right]^{k_1} \times L_{k_1}\left[-\frac{k_{i,j}(k_{i,j} + 1)\gamma}{(k_{i,j} + 1)\gamma + \bar{\gamma}_{i,j}}\right], \quad (7)$$

with $L_n(\cdot)$ denoting the Laguerre polynomial [13, eq. (8.970)].

III. TAS/SD STATISTICS

A. Independent and Non-Identically Distributed Conditions

Assuming i.n.d. fading/shadowing conditions, the CDF of $\gamma_{\ell,\kappa}$ is given by

$$F_{\gamma_{\ell,\kappa}}(\gamma) = 1 - \sum_{i,j=1}^{N_t, N_r} \sum_{\substack{q_{x,y}=1 \\ x,y \neq i,j}}^{\alpha_{x,y}-1} \frac{S_{i,j}}{\Gamma(\alpha_{i,j}) \bar{\gamma}_{i,j}^{-\alpha_{i,j}}} \mathcal{I}(\gamma) \quad (8)$$

where

$$\begin{aligned} \mathcal{I}(\gamma) &= \frac{(h-2)!}{B^{h-1}} \left[1 - \frac{\gamma(k_{\ell,\kappa} + 1)}{B + (k_{\ell,\kappa} + 1)\gamma} \right. \\ &\times \exp\left(-\frac{k_{\ell,\kappa} B}{B + \gamma(k_{\ell,\kappa} + 1)}\right) \sum_{t=0}^{h-2} \left(\frac{B}{B + (k_{\ell,\kappa} + 1)\gamma}\right)^t \\ &\left. \times L_t\left(-\frac{k_{\ell,\kappa} \gamma(k_{\ell,\kappa} + 1)}{B + \gamma(k_{\ell,\kappa} + 1)}\right) \right], \end{aligned} \quad (9)$$

$$\sum_{\substack{q_{x,y}=1 \\ x,y \neq i,j}}^{\alpha_{x,y}-1} = \sum_{q_{1,1}=1}^{\alpha_{1,1}-1} \cdots \sum_{q_{1,N_r}=1}^{\alpha_{1,N_r}-1} \sum_{q_{2,1}=1}^{\alpha_{2,1}-1} \cdots \sum_{q_{x,y}=1}^{\alpha_{x,y}-1} \cdots \sum_{q_{N_t,N_r}=1}^{\alpha_{N_t,N_r}-1},$$

$x \neq i$ OR $y \neq j$

$\sum_{i,j=1}^{N_t N_r} = \sum_{i=1}^{N_t} \sum_{j=1}^{N_r}$, $S_{i,j} = \frac{\prod_{z_1, z_2=1}^{N_t N_r} \bar{\gamma}_{z_1, z_2}^{q_{z_1, z_2}}}{q_{1,1}! \cdots q_{1,N_r}! q_{2,1}! \cdots q_{N_t, N_r}!}$. The proof for (8), due to space limitation is not presented here. The corresponding PDF is given by

$$\begin{aligned} f_{\gamma_{\ell,\kappa}}(\gamma) &= \sum_{i,j=1}^{N_t N_r} \sum_{\substack{q_{x,y}=1 \\ x,y \neq i,j}}^{\alpha_{x,y}-1} \frac{\exp(-k_{\ell,\kappa}) S_{i,j} (k_{\ell,\kappa} + 1)}{\Gamma(\alpha_{i,j}) \bar{\gamma}_{i,j}^{-\alpha_{i,j}} [(k_{\ell,\kappa} + 1)\gamma + B]^h} \\ &\times \Gamma(h) \exp\left(\frac{k_{\ell,\kappa} (k_{\ell,\kappa} + 1)\gamma}{B + (k_{\ell,\kappa} + 1)\gamma}\right) \sum_{t=0}^{h-1} \frac{(1-h)_t}{t!(1)_t} \\ &\times \left(-\frac{k_{\ell,\kappa} (k_{\ell,\kappa} + 1)\gamma}{(k_{\ell,\kappa} + 1)\gamma + B}\right)^t, \end{aligned} \quad (10)$$

where $h = \alpha_{i,j} + \sum_{z_1, z_2=1}^{N_t N_r} q_{z_1, z_2} + 1$, $B = \sum_{i,j=1}^{N_t N_r} \bar{\gamma}_{i,j}$, and $(z)_n$ denotes the pochhammer symbol [14, eq. (6.1.22)]. The total CDF of the output SNR is given by

$$F_{\gamma_{\text{out}}}(\gamma) = \sum_{\ell=1}^{N_t} \sum_{\kappa=1}^{N_r} P_{\ell,\kappa} F_{\gamma_{\ell,\kappa}}(\gamma), \quad (11)$$

in which $P_{\ell,\kappa}$ can be evaluated as

$$P_{\ell,\kappa} = \sum_{\substack{q_{x,y}=1 \\ x,y \neq i,j}}^{\alpha_{x,y}-1} \frac{S_{\ell,\kappa} \bar{\gamma}^{\alpha_{\ell,\kappa}} \Gamma(h-1)}{\Gamma(\alpha_{\ell,\kappa}) B^{h-1}}. \quad (12)$$

The proof of (12), due to space limitation is not presented here.

B. Independent and Identically Distributed Conditions

For i.i.d. fading/shadowing, i.e., assuming that $\alpha_{i,j} = \alpha$, $\bar{\gamma}_{i,j} = \bar{\gamma}$, $k_{i,j} = k$, the CDF expression of γ_{out} is given by

$$\begin{aligned} F_{\gamma_{\text{out}}}(\gamma) &= 1 - \sum_{\substack{n_1, n_2, \dots, n_\alpha=1 \\ n_1 + \dots + n_\alpha = N_{t,r}-1}}^{N_{t,r}-1} \frac{(b-2)!}{\Gamma(\alpha) N_{t,r}^{b-2}} \\ &\times \left\{ 1 - \frac{\gamma(k+1)}{N_{t,r} \bar{\gamma} + (k+1)\gamma} \exp\left[-\frac{k N_{t,r} \bar{\gamma}}{N_{t,r} \bar{\gamma} + \gamma(k+1)}\right] \right. \\ &\times \left. \sum_{t=0}^{b-2} \left[\frac{N_{t,r} \bar{\gamma}}{N_{t,r} \bar{\gamma} + \gamma(k+1)}\right]^t L_t\left[-\frac{k(k+1)\gamma}{N_{t,r} \bar{\gamma} + \gamma(k+1)}\right] \right\}, \end{aligned} \quad (13)$$

where

$$\sum_{\substack{n_1, n_2, \dots, n_\alpha=1 \\ n_1 + \dots + n_\alpha = N_{t,r}-1}}^{N_{t,r}-1} = \sum_{n_1=0}^{N_{t,r}-1} \sum_{n_2=0}^{N_{t,r}-1} \cdots \sum_{n_\alpha=0}^{N_{t,r}-1} \frac{\Gamma(N_{t,r}) / (n_1! \cdots n_\alpha!)}{0! n_1! \cdots (\alpha-1)! n_\alpha!},$$

$N_{t,r} = N_t N_r$, and $b = \sum_{j=2}^{\alpha} (j-1)n_j + \alpha + 1$. For deriving (13), a convenient expression for the PDF of p_{max} is required, which, in general, is defined as $f_{p_{\text{max}}}(y) = N_{t,r} f_{p_{i,j}}(y) F_{p_{i,j}}(y)^{N_{t,r}-1}$. Substituting (4) and

$$F_{p_{z_1, z_2}}(y) = \frac{\Gamma(\alpha_{z_1, z_2} \bar{\gamma}_{z_1, z_2} / y)}{\Gamma(\alpha_{z_1, z_2})} \quad (14)$$

in this definition and employing the multinomial identity, the following simplified expression is extracted

$$f_{p_{\text{max}}}(y) = \frac{N_{t,r}}{\Gamma(\alpha)} \exp\left(-\frac{N_{t,r} \bar{\gamma}}{y}\right) \sum_{\substack{n_1, n_2, \dots, n_\alpha=1 \\ n_1 + \dots + n_\alpha = N_{t,r}-1}}^{N_{t,r}-1} \frac{\bar{\gamma}^{b-1}}{y^b}. \quad (15)$$

Based on (15) and using a similar approach as the one used for deriving (8), finally yields (13). The corresponding expression for the PDF of γ_{out} is given by

$$\begin{aligned} f_{\gamma_{\text{out}}}(\gamma) &= \frac{N_{t,r}}{\Gamma(\alpha)} \sum_{\substack{n_1, n_2, \dots, n_\alpha=1 \\ n_1 + \dots + n_\alpha = N_{t,r}-1}}^{N_{t,r}-1} \exp\left[\frac{k(k+1)\gamma}{N_{t,r} \bar{\gamma} + (k+1)\gamma}\right] \\ &\times \frac{(k+1)\Gamma(b) \bar{\gamma}^{b-1} e^{-k} \sum_{p=0}^{b-1} (1-b)_p \left[\frac{-k(k+1)\gamma}{N_{t,r} \bar{\gamma} + (k+1)\gamma}\right]^p}{(N_{t,r} \bar{\gamma} + (k+1)\gamma)^b p!(1)_p}. \end{aligned} \quad (16)$$

IV. PERFORMANCE ANALYSIS AND NUMERICAL RESULTS

The performance of the proposed system is investigated using the criterion of OP. The OP is defined as the probability that the output SNR falls below a predetermined threshold γ_T and it can be evaluated as $P_{\text{out}} = F_{\gamma_{\text{out}}}(\gamma_T)$, in which $F_{\gamma_{\text{out}}}(\gamma_T)$ is given by (11), for the i.n.d. scenario, and by (13), for the i.i.d. scenario.

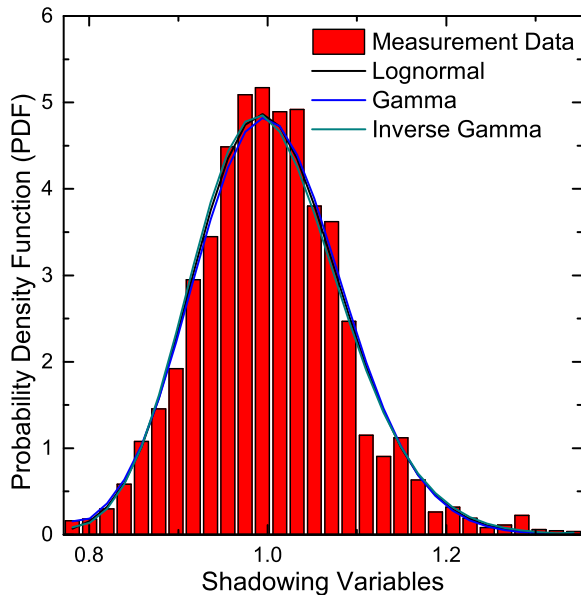


Fig. 1. Empirical and theoretical PDFs comparisons.

A. Numerical Results

First, the appropriateness of the IG distribution to model shadowing effects was studied. To this aim, the empirical data obtained in the channel measurement campaign presented in [15] are employed. These data were collected in an urban pedestrian propagation environment with a stationary Tx and a mobile Rx, resulting in time-variant channel characteristics. In Fig. 1, the empirical PDF of the signal envelope mean (shadow fading) is plotted. In the same figure, for comparison purposes, the corresponding PDFs of Gamma, IG, and lognormal distributions are also plotted, using the method of moments to estimate their parameters. It is shown that all PDFs provide excellent fit to the empirical one. Moreover, in order to more clearly understand which distribution fits better to the measured data, the Kullback-Leibler divergence criterion is used [16]. According to this, the distribution that provides the best fit to the measured data is the one with the minimum value for the distance d_{KL} . Our analysis showed that $d_{KL} = 1.8, 1.54, 1.7\%$, for Gamma, IG, and lognormal distributions, respectively. Therefore, it is shown that the IG distribution can be an excellent model for shadow fading in time-varying channel conditions.

In Fig. 2, assuming $k = 4, \alpha = 2, \bar{\gamma} = 0\text{dB}$, the normalized OP is plotted as a function of the outage threshold, γ_T , for different numbers of Tx and Rx antennas. It is shown that as the number of the antennas increases, the performance improves with a decreased rate. Moreover, a clear performance improvement is achieved with the proposed scheme, as compared to the SISO scenario (with shadowing), where random AS is performed. It is noteworthy that the proposed scheme can

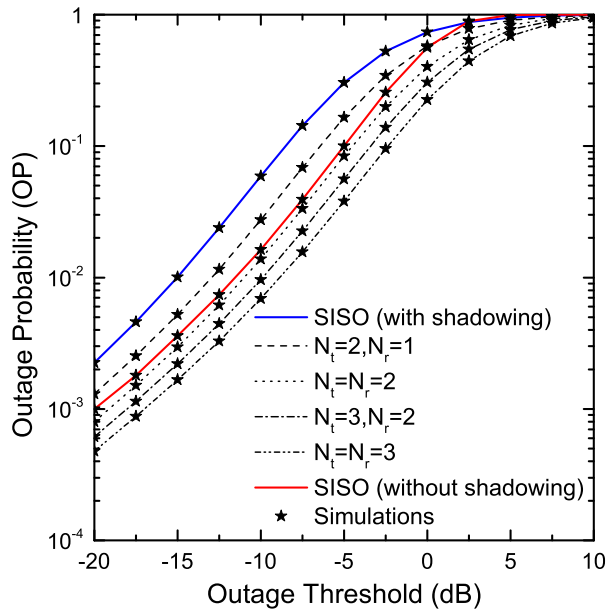


Fig. 2. Normalized OP as a function of the outage threshold.

be considered as an effective shadowing countermeasure technique, since for scenarios with $N_t, N_r \geq 2$, it provides better performance as compared to a SISO system operating in a non-shadowed environment.

Another important investigation that is also performed concerns the performance comparison between SI- and CSI-based AS schemes, with the latter one employing outdated versions of CSI. In order to do so, the CDF of the output SNR of a CSI-based TAS scheme operating over Rice/IG composite fading environment is required to be evaluated. An exact analytical expression for this CDF has been derived, which due to space limitation, is not presented here. In Fig. 3, assuming $\alpha = 3$, the OP of the proposed scheme and the one that is based on outdated CSI is plotted as a function of the temporal correlation coefficient ρ_t , which quantifies the correlation between the exact and the outdated versions of the received SNR. To obtain this figure, the following assumption was made $N_t = 2, N_r = 1$, while three different scenarios regarding the fading/shadowing conditions were considered and presented in the Table included in Fig. 3. It is shown that the performance of the CSI-based system improves as ρ_t increases as well as with an increase of k . A general observation is that for reasonable values of the time correlation, i.e., $\rho_t > 0.6$, which corresponds to typical relative velocities, the CSI-based TAS scheme offers better performance in the cases where strong fading effects are present. A reason for this behaviour is that in these scenarios the multipath components are dominant compared to the constant term of the Rice model and thus the technique that offers improved fading countermeasure performance is the one that focuses on the selection of the best fading variable,

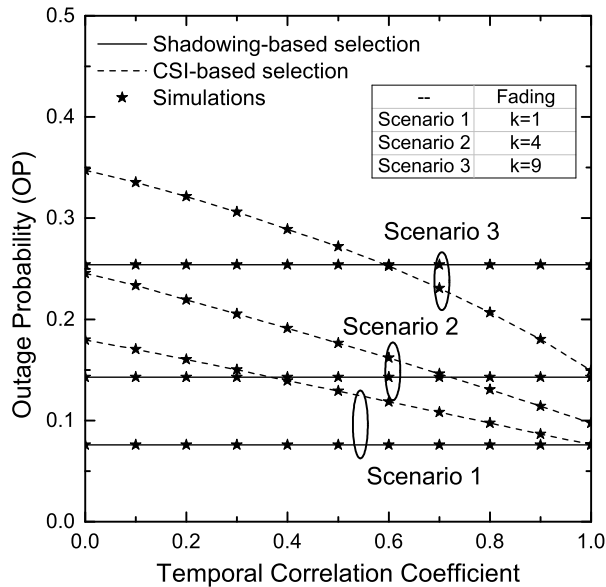


Fig. 3. Outage probability as a function of the correlation coefficient for SI-, CSI-based antenna selection schemes.

i.e., the CSI-based scheme. However, it is noteworthy that the proposed scheme outperforms the one that is based on outdated CSI in all other investigated scenarios, where mild fading conditions and/or lower values of ρ_t exist, which correspond to high velocities. More specifically, for mild fading conditions, i.e., scenarios 2 and 3, the proposed scheme provides better performance for almost the entire region of ρ_t . These results reveal that the negative impact of outdated CSI on the system's performance can be alleviated by exploiting the shadowing information. Finally, the Monte Carlo simulations that were included in Figs. 2 and 3 verify the validity of the presented theoretical framework.

V. CONCLUSIONS

The performance of a TAS/SD scheme operating in a V2V communication environment in the presence of composite fading has been analytically investigated. A new AS scheme is proposed in which the antenna selection at both Tx and RX is performed by exploiting the stationarity of the large scale fading. Capitalizing on the slow variations of the shadowing variable, the detrimental consequence of the outdated CSI that is frequently observed in V2V communications is counteracted. The results presented are based on the derived theoretical analysis, simulations, and empirical data. We have shown the appropriateness of the inverse gamma distribution to model the large scale effects as well as the impact of outdated CSI on the system's performance. Moreover, it was also shown that in practical situations the proposed approach outperforms the one that exploits CSI acquisition, under various fading/shadowing conditions.

ACKNOWLEDGEMENT

The publication of this paper has been partly supported by the University of Piraeus Research Center.

REFERENCES

- [1] Y. Li *et al.*, "A channel quality metric in opportunistic selection with outdated CSI over Nakagami- m fading channels," *IEEE Trans. Veh. Technol.*, vol. 61, no. 3, pp. 1427–1432, Mar. 2012.
- [2] P. S. Bithas *et al.*, "On the double-generalized gamma statistics and their application to the performance analysis of V2V communications," *IEEE Trans. Commun.*, vol. 66, no. 1, pp. 448–460, Jan. 2018.
- [3] A. Yilmaz, F. Yilmaz, M. S. Alouini, and O. Kucur, "On the performance of transmit antenna selection based on shadowing side information," *IEEE Trans. Veh. Technol.*, vol. 62, no. 1, pp. 454–460, Jan. 2013.
- [4] S. Hessian *et al.*, "On the secrecy enhancement with low-complexity large-scale transmit selection in MIMO generalized composite fading," *IEEE Wireless Commun. Lett.*, vol. 4, no. 4, pp. 429–432, Aug. 2015.
- [5] E. Erdogan, A. Afana, and S. Ikki, "Multi-antenna downlink cooperative systems over composite multipath/shadowing channels," in *IEEE Wireless Communications and Networking Conference (WCNC)*, Mar. 2017.
- [6] D. Vlastaras *et al.*, "Impact of a truck as an obstacle on vehicle-to-vehicle communications in rural and highway scenarios," in *IEEE 6th International Symposium on Wireless Vehicular Communications (WiVeC)*, Sep. 2014.
- [7] Q. Wang, D. W. Matolak, and B. Ai, "Shadowing characterization for 5-GHz vehicle-to-vehicle channels," *IEEE Trans. Veh. Technol.*, vol. 67, no. 3, pp. 1855–1866, Mar. 2018.
- [8] S. K. Yoo *et al.*, "The K- μ /inverse gamma fading model," in *IEEE 26th Annual International Symposium on Personal, Indoor, and Mobile Radio Communications (PIMRC)*, 2015, pp. 425–429.
- [9] S. K. Yoo and S. L. Cotton, "Composite fading in non-line-of-sight off-body communications channels," in *11th European Conference on Antennas and Propagation (EUCAP)*, Mar. 2017, pp. 286–290.
- [10] L. S. Muppirisetty, T. Svensson, and H. Wymeersch, "Spatial wireless channel prediction under location uncertainty," *IEEE Trans. Wireless Commun.*, vol. 15, no. 2, pp. 1031–1044, Feb. 2016.
- [11] T. Abbas, K. Sjöberg, J. Karedal, and F. Tufvesson, "A measurement based shadow fading model for vehicle-to-vehicle network simulations," *International Journal of Antennas and Propagation*, 2015.
- [12] M. K. Simon and M.-S. Alouini, *Digital Communication over Fading Channels*, 2nd ed. New York: Wiley, 2005.
- [13] I. S. Gradshteyn and I. M. Ryzhik, *Table of Integrals, Series, and Products*, 6th ed. New York: Academic Press, 2000.
- [14] M. Abramowitz and I. A. Stegun, *Handbook of mathematical functions: with formulas, graphs, and mathematical tables*. Courier Corporation, 1964, vol. 55.
- [15] V. Nikolaidis, N. Moraitis, and A. G. Kanatas, "Dual-polarized narrowband MIMO LMS channel measurements in urban environments," *IEEE Trans. Antennas Propag.*, vol. 65, no. 2, pp. 763–774, Feb. 2017.
- [16] S. Kullback and R. A. Leibler, "On information and sufficiency," *The annals of mathematical statistics*, vol. 22, no. 1, pp. 79–86, 1951.